

# Pressure drop, flow pattern and local water volume fraction measurements of oil-water flow in pipes

W A S Kumara, B M Halvorsen and M C Melaaen

Telemark University College, PO. Box 203, N-3901, Porsgrunn, NORWAY

E-mail: Morten.C.Melaaen@hit.no

**Abstract.** Oil-water flow in horizontal and slightly inclined pipes was investigated. The experimental activities were performed using the multiphase flow loop at Telemark University College, Porsgrunn, Norway. The experiments were conducted in a 15 m long, 56 mm diameter, inclinable steel pipe using Exxsol D60 oil (density of  $790 \text{ kg/m}^3$  and viscosity of  $1.64 \text{ mPa s}$ ) and water (density of  $996 \text{ kg/m}^3$  and viscosity of  $1.00 \text{ mPa s}$ ) as test fluids. The test pipe inclination was changed in the range from  $5^\circ$  upward to  $5^\circ$  downward. Mixture velocity and inlet water cut varies up to 1.50 m/s and 0.975, respectively. The time averaged cross sectional distributions of oil and water were measured with a single-beam gamma densitometer. The pressure drop along the test section of the pipe was also measured. The characterization of flow patterns and identification of their boundaries are achieved via visual observations and by analysis of local water volume fraction measurements. The observed flow patterns were presented in terms of flow pattern maps for different pipe inclinations. In inclined flows dispersions appear at lower mixture velocities compared to the horizontal flows. Smoothly stratified flows observed in the horizontal pipe disappeared in upwardly inclined pipes and new flow patterns, plug flow and stratified wavy flow were observed. The water-in-oil dispersed flow regime slightly shrinks as the pipe inclination increases. In inclined flows the dispersed oil-in-water flow regime extended to lower mixture velocities and lower inlet water cuts. The present experimental data were compared with results of a flow pattern dependent prediction model, which uses the area averaged steady state two-fluid model for stratified flow and the homogeneous model for dispersed flow. The two-fluid model was able to predict the pressure drop and water hold-up for stratified flow. The homogeneous model was not able to predict the pressure profile of dispersed oil-water flow at higher water cuts. The two-fluid model and homogeneous model over-predicts the pressure drop for dual continuous flow.

**Keywords:** Oil-water flow, gamma densitometry, pressure drop, flow patterns, water cut

## 1. Introduction

Oil-water flows have many applications in a diverse range of process industries and particularly in the petroleum industry. Increased offshore oil and gas exploration and production have resulted in transportation of well fluids in pipelines over relatively long distances. Often, the fluid delivered by the well contains water, which is already present within the stratum. In early days, the amount of free water produced was small and hence given a little attention. However, in recent years, oil extraction by drilling of horizontal or nearly horizontal wells is often accompanied with a high water throughput, due to the presence of water in old wells or injection of water into the wells for a better oil extraction. Today, oil well might be economical to operate even for water cuts as high as 0.90. The influence of the water phase with respect to the pressure drop is of particular importance for oil fields operating at high water cuts and low wellhead pressures. Therefore optimisation of pipeline operations for transport of these fluids requires the knowledge of the pressure drop and in situ distribution of the

liquids. There was an initial interest in oil-water flows relevant to petrochemical industries during 1950s and 1960s (Russel et al., 1959; Charles et al., 1961), mainly concerned with improving pumping requirements during viscous oil transportation by introducing water in the pipelines. After a relatively quiescent period, interest in the field is now growing rapidly because of the simultaneous production of oil and water from many currently operating oil fields.

In the pipe flow of oil and water, different shapes and spatial distributions of their deformable interface can appear which are commonly called flow regimes or flow patterns. A great deal of efforts has gone into investigating and classifying flow regimes occurring under various flow conditions and the usual outcome is to express results in terms of “flow pattern map”. Previous investigations in this area have been reviewed extensively by Valle (1998). In oil-water flow systems, oil properties can be quite diverse, and the oil-water viscosity ratio can vary from more than a million to less than one, and its rheological behaviour can be Newtonian or non-Newtonian. Hence, the available data do not show evidence of general agreement among the different flow patterns observed. In early experimental studies of oil-water flow in horizontal pipes, Oglesby (1979) has reported 14 different flow patterns, whereas others described only three to four different flow patterns (Russel et al., 1959; Malinowsky, 1975). Since the 1990s, with the development of advanced instruments and techniques in multiphase flow measurements, different flow pattern parameters have been measured more accurately and flow patterns of oil-water flow have been analyzed objectively (Angeli, 1996; Nädler et al., 1997; Trallero et al., 1997). At low mixture velocities the less dense phase, oil, flows over the denser phase, water, with a clearly defined interface. This flow regime is named as stratified flow. The dispersed flow pattern where one phase is dispersed as droplets into the continuum of the other phase will appear at higher mixture velocities. At intermediate mixture velocities a combination of these two flow regimes can appear where both fluids can be dispersed, at various degrees, into the continuum of the other.

The introduction of a small inclination in the pipeline, as well as the size of the inclination, will affect the boundaries between the flow patterns observed in horizontal flows (Lum et al., 2006). In inclined oil-water flows the gravitational force has components both normal and parallel to the pipe axis. The normal component promotes the segregation of the phases as in the horizontal flow, while the parallel one can act either in the direction of the flow (downwardly inclined flow) or in the opposite direction (upwardly inclined flow). Hence, the downward inclination of the pipe causes higher in situ water velocities than in the corresponding horizontal case; conversely, the in situ water velocity in an upwardly inclined pipe is lower than the horizontal pipe. These differences in velocities and phase hold-up cause changes in the flow patterns and other flow properties measured in inclined oil-water flows compared to the horizontal flows. In upwardly inclined flow dispersion appears at lower velocities than in the horizontal flow (Oddie et al., 2003; Lum et al., 2004). Hence, the transition from stratified to dual continuous flow occurs at low mixture velocities in upwardly inclined flows compared to the horizontal flows. Abduvayt et al. (2004) at  $+3^\circ$  and Scott (1985) at  $+15^\circ$  and  $+30^\circ$  observed that the smooth interface of horizontal flow was completely replaced by large amplitude waves at low mixture velocities. In contrast Alkaya (2000) reported a very smooth interface in oil-water flows at  $+1^\circ$  and  $+5^\circ$ . There is no consensus on the effect of upward inclination at higher mixture velocities, namely on the dual continuous flow and fully dispersed flow (Lum et al., 2004). Numerous experimental investigations have been performed on flow patterns of oil-water flow in downwardly inclined pipes. In general, Cox (1985) and Alkaya (2000) observed that the transition from separated to dispersed flow occurs at lower mixture velocities in downwardly inclined pipes compared to the horizontal flow. Alkaya (2000) reported that downward inclination enhance the dispersed water-in-oil flow pattern slightly so that it appears at lower mixture velocities at  $-5^\circ$ . Stratified wavy flow pattern has been observed by Abduvayt et al. (2004) and Rodriguez et al. (2006).

For two-phase oil-water pipe flow the pressure drop behavior with respect to oil-water ratio has been presented in a number of publications starting with the work of Charles et al. (1961). The conclusions drawn from the respective studies vary considerably and it is difficult to derive a consistent behaviour. The results depend critically on the fluid properties, pipe geometry and flow patterns. For oils with medium and high viscosity, pressure drop in stratified flow decreases monotonically with increasing

water fraction from single-phase oil to single-phase water (Guzhov et al., 1973; Nädler et al., 1997). For high viscosity and low density difference, an annular water film is formed on the walls and the pressure drop becomes very low as described by Charles et al. (1961). For oil having viscosities in the order of water (or slightly above) the pressure drop in stratified flow is approximately constant and changes only slightly with oil-water ratio, dependent upon the viscosities and densities (Valle et al., 1997). It has been established from rheological studies of dispersions that the relative viscosity, with respect to the continuous phase, increases for increasing fraction of the dispersed phase. The consequence is that the pressure drop increases gradually towards the phase inversion point for oil continuous dispersion and decreases from the phase inversion point to single-phase water flow (Valle, 1998). The phase inversion point is defined as the volume fraction of the dispersed phase above which this phase will become continuous (Angeli et al., 1998). Guzhov et al. (1973), Angeli et al. (1998) and Valle et al. (1997) observed a peak in pressure drop and it was attributed to the phase inversion phenomena. In similar experiments Nädler et al. (1997) found two peaks in the pressure gradient. They related the first to the transition from water-in-oil dispersed flow to stratified-dispersed flow and the second to the transition from stratified-dispersed flow to an oil-in-water dispersed flow. Elseth (2001) observed a peak in measured pressure drop of oil-water flow in horizontal pipes at higher water cuts. It was related to the dispersion effect of the oil layer at higher water cuts.

Most of the previous studies mainly identify the flow patterns and investigate pressure drop variations of oil-water flows. Phase fraction distribution data were seldom measured (Trallero et al., 1997). However, the water volume fraction measurements are of considerable technical importance in two-phase oil-water flow systems as it is a key parameter in the prediction of frictional pressure drop. Furthermore, the overall water hold-up is related to the local phase fraction measurements. Therefore some effort has been devoted to investigate phase distributions in oil-water flows. The phase distribution in oil-water flows can be identified by the electrical methods due to the differences in conductivity and permittivity between phases. High frequency impedance probes are used to measure mean water volume fractions in oil-water flow because of the large dielectric constant contrast between the two liquids (Vigneaux et al., 1988). Since one phase (water) is conductive and the other is non-conductive (oil), the conductivity probes were used to ascertain phase distribution of oil-water flow by Angeli et al. (1998). Huang et al. (2007) used a capacitance probe to measure water hold-up based on water layer thickness in oil-water flow in horizontal pipes. Oddie et al. (2003) measured water hold-up in oil-water flow using quick-closing valves (QCV). Among the many available techniques, those based on radiation techniques (neutron, gamma and X-ray) appear to be attractive in many multiphase flow applications, because they are non-intrusive and in general, quite reliable (Chan et al., 1981). The gamma and X-ray attenuation techniques have been widely used to investigate gas-liquid flow systems and rarely applied on liquid-liquid flows. Valle et al. (1997) and Elseth (2001) have used gamma densitometry to ascertain phase distribution in oil-water flows in horizontal pipes.

To get a better understanding of oil-water flow more detailed measurements are needed. This paper presents measurements of cross-sectional liquid distribution and pressure drop of two-phase oil-water flow in pipes. The different flow patterns observed in oil-water flow in horizontal and slightly inclined pipes are discussed in detail and presented in terms of flow pattern maps. The results are also compared with published oil-water flow studies. The new experimental data are compared with results of a flow pattern dependent prediction model, which uses the area averaged steady state two-fluid model for stratified flow and the homogeneous model for dispersed flow.

## **2. Experimental set-up**

The experiments were performed in the multiphase flow facility at Telemark University College in Porsgrunn, Norway.

### *2.1. Multiphase flow loop*

A simplified flow sheet of the experimental rig is shown in figure 1. The experiments were performed using Exxsol D60 oil and water at room temperature and atmospheric outlet pressure. The physical

properties of the test fluids are shown in table 1. Oil and water were stored in separate tanks (T100 and T101 for oil and water, respectively) and circulated using volumetric pumps P100 and P101. The mass flow, density and temperature were measured for each phase before entering the test section using Coriolis flow meters (FT109B, FT110, FT114B and FT115). The oil and water phases are introduced into the test section via a modified Y-junction, which ensures minimum mixing as shown in figure 2. The phases are fed into the pipeline in layers corresponding to their densities resulting in a stratified flow just behind the inlet section. The oil is introduced at the top and water at the bottom. A plate separates both phases until the entrance to the test section. This design has been selected to prevent the formation of emulsions due to the mixing effect taking place in the entrance section. The test section is a 15 m long steel pipe (wall roughness  $10^{-5}$  m) with inner diameter equal to 56 mm. The test pipe inclination can be changed in the range from  $5^\circ$  upward to  $5^\circ$  downward. In the test section, inlet pressure and the pressure drop over two distances were measured. Towards the end of the test section, there is a short transparent section for visual observations. The oil-water mixture flows along the test section 11.3 m from the entry point, before the gamma densitometer, providing a sufficient entrance length to stabilize the flow. After the gamma densitometer, a 3.7 m long pipe section is provided to avoid exist effects on the measurements. Downstream of the test section a 76.2 mm stainless steel pipe is installed to pre-separate the fluids before entering into the oil-water separator (R100). In the separator, the oil-water mixture is separated before entering to the storage tanks. A controller based on LabView<sup>®</sup> allowed to set the input oil and water flow rates and to select the appropriate pumps and flow meters.

**Table 1.** Properties of the liquids at 25 °C and 1 atm.

Liquid	Exxsol D60 oil	Water
Density [kg/m <sup>3</sup> ]	790	996
Viscosity [mPa s]	1.64	1.00
Surface tension [mN/m <sup>2</sup> ]	25.30	71.97
Interfacial tension [mN/m <sup>2</sup> ]	43.00	

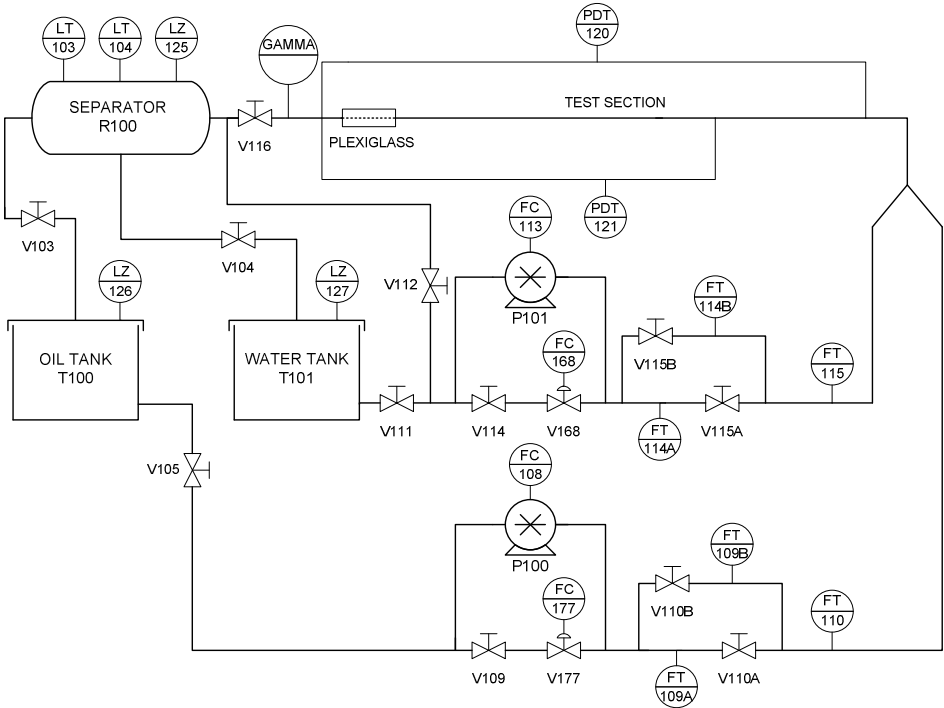


**Figure 1.** Simplified flow sheet of the test rig.

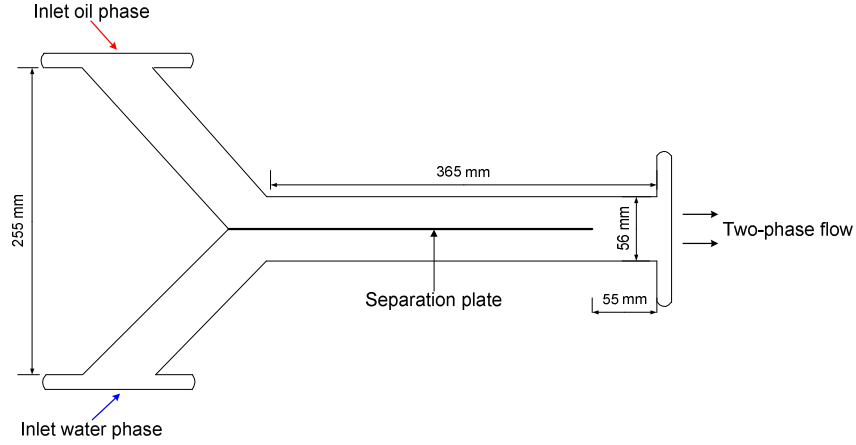


**Figure 2.** The inlet mixing unit.

## 2.2. Gamma densitometry

The basic principle of the gamma densitometry is the experimentally observed fact that the intensity of a collimated gamma beam decreases exponentially as it goes through matter. The intensity of a monoenergetic gamma beam that is transmitted through a homogeneous material is governed by the Beer-Lambert's law which can be expressed as:

$$I = I_0 \exp(-\rho\mu x) \quad (1)$$

where  $I_0$  is the incident intensity of the gamma beam and  $I$  is the intensity of the beam detected after the beam has travelled a distance  $x$  through the absorbing medium. The capability of material to absorb gamma radiation is characterized by its mass absorption coefficient  $\mu$ , and  $\rho$  represents the density of the material. The basic equation can be applied to an oil-water two-phase system with mass absorption coefficients  $\mu_o$  and  $\mu_w$  and densities  $\rho_o$  and  $\rho_w$ , respectively, the corresponding expression is:

$$I = I_0 \exp[-(\rho_o\mu_o x_o + \rho_w\mu_w x_w)] \quad (2)$$

where  $x_o$  and  $x_w$  are the path lengths of the beam in the oil and water phases, respectively. In terms of the measured intensities,  $I_{o/w}$ ,  $I_o$  and  $I_w$  corresponding to the test section filled with the two-phase oil-water mixture, pure oil and pure water, respectively, the chordal averaged water volume fraction, ( $\varepsilon_w$ ), is estimated from (Chaoki et al., 1997):

$$\varepsilon_w = \frac{\ln[I_{o/w} / I_o]}{\ln[I_w / I_o]} \quad (3)$$

This expression is applicable only in two-phase systems and only when a narrow collimated beam is used in the measurement process. In principle, the water volume fraction profile in oil-water flow can be determined to a fine detail by having a source emitting narrow beam of radiation and an opposing detector scan across the cross-section. This yields a series of chordal averaged measurements.

In the present work, a single-beam gamma densitometer operated in the count mode is used to obtain information about the local phase fractions in oil-water flow. The major components of the gamma densitometer are shown in figure 3. The device consist of a sealed gamma source (45 mCi, Am-241), beam collimators, a scintillator detector (NaI crystal doped with thallium) and a signal processing system. The signal processing system includes a photomultiplier tube and associated electronics. The gamma radiation emission is isotropic process and fine collimator structure must be used to generate a narrow beam. In the present system, 3 mm circular slot is used as the source collimator. A short polypropylene pipe section is used for gamma densitometry measurements. The source is located at one side of the pipe and sends a gamma beam towards the detector located at the opposite side of the pipe. The detector is also collimated so that only transmitted radiation will be detected whereas scattered radiation can be neglected. The detector collimator is a rectangular slot (3x10 mm). Genie 2000 VDM software is used for acquisition, display and analysis of gamma densitometry data. The main components of the signal processing system of the single-beam gamma densitometer are shown

in figure 4. During the operation, the scintillator crystal absorbs energy from the detected gamma radiation and produces a proportional flash of light. The light flash causes the photomultiplier tube cathode to emit a proportional quantity of electrons. These are attracted from dynode to dynode through the photomultiplier tube with a multiplication effect at each successive dynode due to secondary emission. The highly intensified burst of electrons which arrives at the anode of the tube, still proportional to the energy of origin, is transferred to form a change at the input capacitor in the preamplifier. The preamplifier responds by creating a positive output pulse which remains the basic proportional significance. The preamplifier is built together with photomultiplier tube. There are two inputs to the preamplifier. The anode output from the photomultiplier tube and the high voltage supply. The high voltage supply can furnish an output of  $\pm 1-1000$  V DC. The output signal of the preamplifier has amplitude depending on the input pulse and the high voltage supply. Figure 5(a) depicts the typical output signal from the preamplifier. The signal from the preamplifier is fed into a delay line amplifier. It produces 100 ns long pulses from the exponential decaying pulses. Hence, the “chaos” from the preamplifier is turned into a sequence of pulses with different amplitudes, by adding 100 ns delayed inverted copy of the original pulse as shown in figure 5(b). After the delay line amplifier, a Single Channel Analyser (SCA) uses a discriminating window, consisting of a lower and upper voltage level, to filter this signal, in order to produce a logic output pulse for every incoming

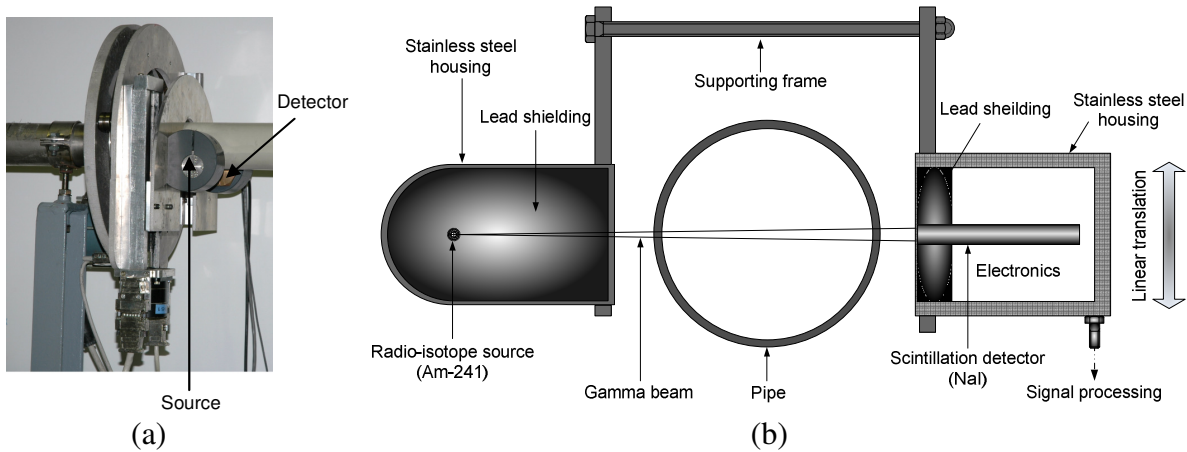


**Figure 3.** The single-beam gamma densitometer: (a) Gamma densitometer set-up, (b) Schematic design of gamma densitometer.

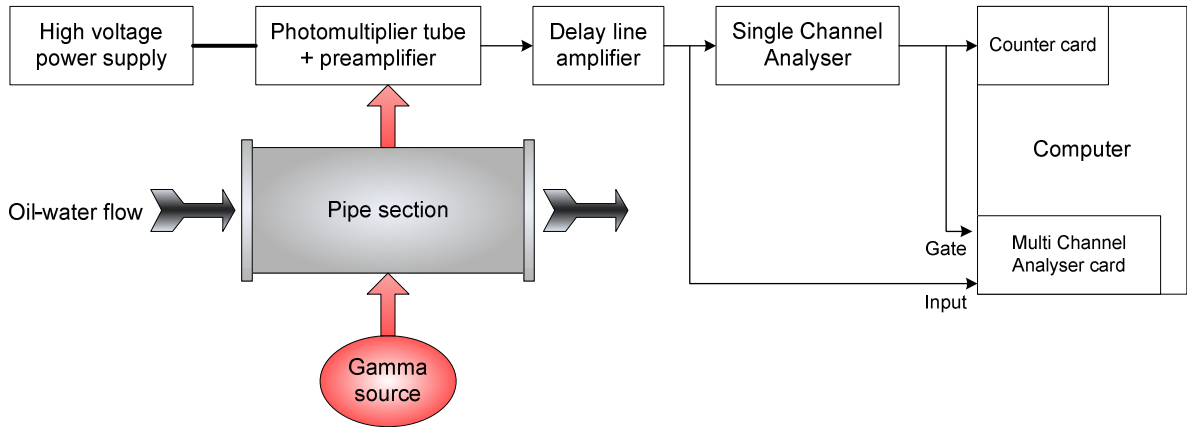


**Figure 4.** Signal processing system of the single-beam gamma densitometer.

signal resulting from a photon of a particular energy. The SCA produces a logic output pulse if a pulse from the delay line amplifier is higher than the low level of the window and lower than the high level of the window. Figure 5(c) shows the logic output generated by SCA. The gamma source emits photons at a range of energies. The background radiation produces low frequency scatter. In the entire range of frequencies detected by the photomultiplier tube, the dominant energy is the energy of the photon that is produced by the decaying process of Am-241 that is 59.5 keV. The dominant peak can be isolated with the electrical circuit producing measurements at a single energy level. However, nuclear sources may have a second or third less pronounced peak. A Multi Channel Analyzer (MCA) is used to find the number of photons emitted per second at every energy level. Figure 5(d) shows an example of a possible division of photons per frequency interval, the two dashed lines indicate the part of the spectrum that are isolated and used for the measurements. The Multi Channel Analyzer is a PC containing an ORTEC TRUMP-PCI pulse height analyzer card run by the MAESTRO-32 MCA Emulation software package.

Photon count recording is initiated when the steady flow conditions are attained. As with all radiation measurement techniques, because of the statistical nature of the source there is a compromise between measurement time and accuracy. The greater the accuracy required, the longer would be the measurement period. In the present work, photon count data collection is undertaken for a period of

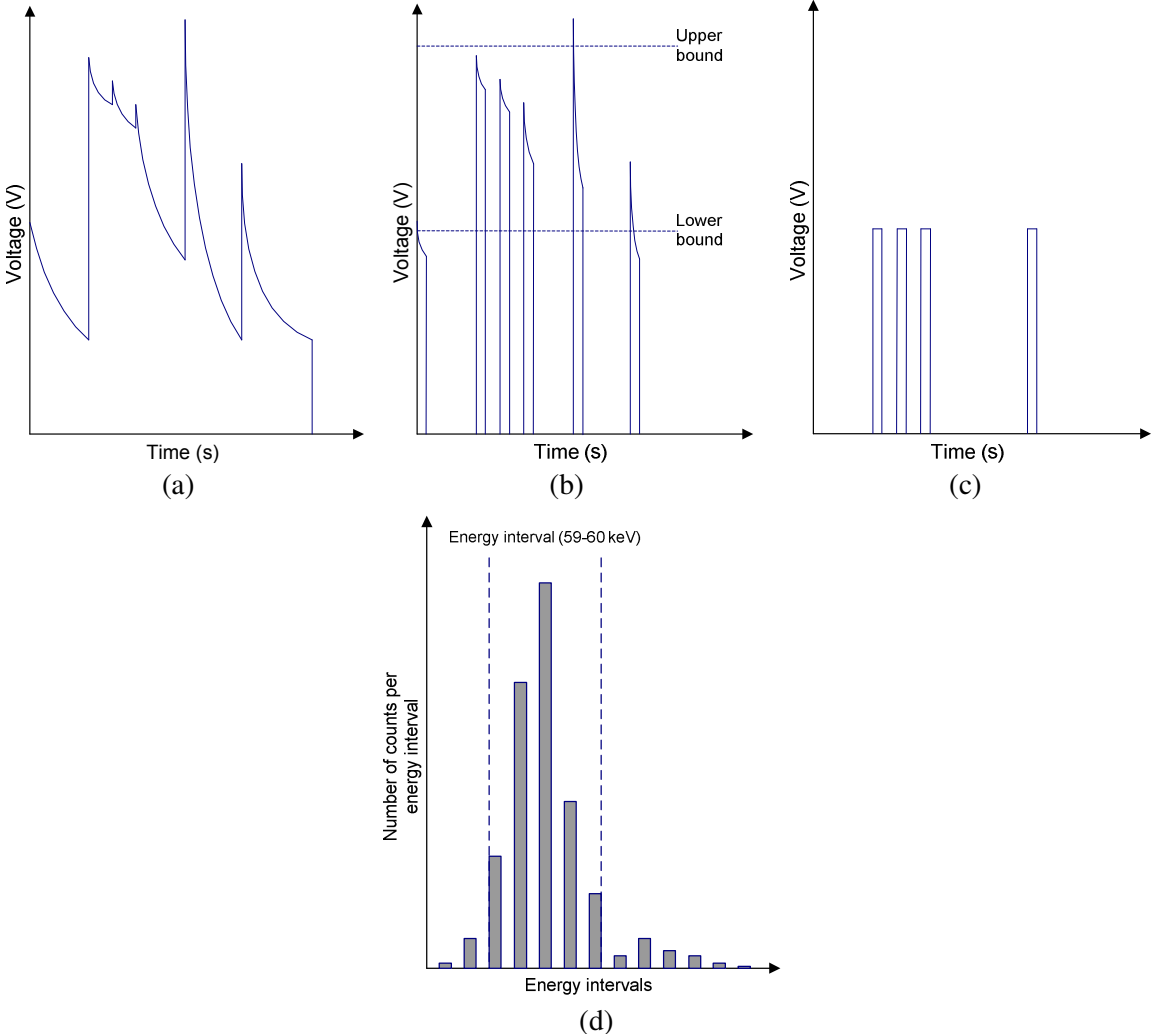


**Figure 5.** Steps in the signal processing of the gamma densitometer results: (a) Output preamplifier, (b) Output delay-line amplifier, (c) Output SCA (logic pulses), (d) Output MCA.

50 seconds at each measurement site. In the experiments the vertical interface position was measured by traversing horizontal gamma beams. Therefore the measurements can not discriminate between waves, interfacial curvature and droplet entrainment.

### 2.3. Investigated flow conditions

The effect of changes in mixture velocity, inlet water cut and pipe inclination on oil-water flow were investigated. The mixture velocity for oil-water flow is defined as:

$$U_m = \frac{Q_o + Q_w}{A} \quad (4)$$

where  $Q_o$  and  $Q_w$  are the inlet volumetric flow rates of oil and water phases, respectively and  $A$  is the pipe cross-sectional area. The inlet water cut,  $\lambda_w$  is defined by:

$$\lambda_w = \frac{Q_w}{Q_w + Q_o} \quad (5)$$

In the present work, four different mixtures velocities (0.25, 0.50, 1.00 and 1.50 m/s) were used. The water cut was varied from 0.025 to 0.975. Pipe inclination,  $\zeta$ , is given in degrees from horizontal where positive inclinations give upward flow and negative inclinations give downward flow. The experiments were performed at different pipe inclinations ( $-5^\circ$ ,  $-1^\circ$ ,  $0^\circ$ ,  $+1^\circ$  and  $+5^\circ$ ).

### 3. Flow pattern dependent prediction models

Two-phase oil-water flow modelling started in a very empirically oriented way, typically based on semi-homogeneous models applying two-phase multipliers and a rich variety of correlations. Charles et al. (1966) used the similarity method developed by Lockhart et al. (1949) for gas-liquid flow, to predict pressure gradient data in stratified flow of two liquids when the one was in laminar and the other in turbulent flow. The two-fluid model developed by Taitel et al. (1976) for gas-liquid flows was used to calculate the pressure drop of stratified oil-water flows by Brauner et al. (1989). This kind of model is also discussed by Valle et al. (1997), Angeli et al. (1998) and Rodriguez et al. (2006). Oil and water were represented as two separate regions and empirical correlations were used for the wall and the interfacial shear stresses. For dispersed oil-water flow the most common prediction method is the homogeneous no-slip model. In this model, the mixture of two fluids is treated as a ‘pseudofluid’ with suitably averaged properties that obeys the usual equations of single-phase flow (Angeli et al., 1998). The homogeneous model has been used to predict the pressure drop in liquid-liquid flows (Valle et al., 1997; Elseth, 2001; Rodriguez et al., 2006). In the present work, the models applied for pressure drop and hold-up predictions are the area-averaged steady state one-dimensional two-fluid model for stratified flow and the homogeneous model for dispersed flow. These models are valid for extreme flow situations of complete phase separation and complete mixing, respectively. However, the comparisons are thought to provide valuable guidelines on the applicability and prediction accuracies when these simple models are used for intermediate flow conditions.

In the two-fluid model the flow parameters are estimated from the combined momentum equations for steady-state flow. Thus, eliminating the pressure drop from the momentum equations of each phase (Angeli et al., 1998; Rodriguez et al., 2006):

$$-\frac{\tau_w S_w}{A_w} + \frac{\tau_o S_o}{A_o} \pm \tau_i S_i \left( \frac{1}{A_w} + \frac{1}{A_o} \right) - (\rho_w - \rho_o)g \sin \xi = 0 \quad (6)$$

where  $A_o$  and  $A_w$  are the cross sectional areas of the oil and the water phase, respectively,  $\tau_o$  and  $\tau_w$  are the wall shear stresses for the oil and the water phases, respectively,  $\tau_i$  is the interfacial shear stress,  $S_o$  and  $S_w$  are the oil-wetted and water-wetted wall peripheries, respectively, and  $S_i$  is the interfacial periphery where  $\tau_i$  acts on. The upper sign of the interfacial shear stress term corresponds to the upper phase (oil) flowing faster than the bottom phase (water). Equation (6) is a non-linear equation which can be solved for the liquid level or hold-up using a standard numerical method if the shear stresses are expressed in terms of known friction factors. The additional relationships required for estimating



geometric parameters and the closure relations for wall and interfacial shear stresses can be found in Angeli et al. (1998) and Rodriguez et al. (2006). The pressure gradient is subsequently calculated by inserting the calculated hold-up values into the one-dimensional differential equations of momentum for oil or water.

The homogeneous model for the pressure gradient in liquid-liquid dispersion is often given as:

$$\frac{dp}{dx} = -\frac{f_m \rho_m U_m^2}{2D} - \rho_m g \sin \xi \quad (7)$$

where  $f_m$  is the mixture friction factor,  $\rho_m$  is the mixture density and  $D$  is the diameter of the pipe. The mixture density is modelled as:

$$\rho_m = \eta_w \rho_w + (1 - \eta_w) \rho_o \quad (8)$$

Here  $\eta_w$  is defined as the water hold-up and it is defined as:

$$\eta_w = \frac{A_w}{A} \quad (9)$$

The main problem in applying this approach is in the calculation of the effective mixture viscosity, particularly since the viscosity can have anomalous behavior during liquid-liquid flow. Since, the present work was not concerned about the phase inversion and the mixture viscosity was simply treated using the homogenous relation as given below (Elseth, 2001):

$$\mu_m = \eta_w \mu_w + (1 - \eta_w) \mu_o \quad (10)$$

The pressure gradient prediction depends on the flow pattern and the accuracy of the water hold-up predictions. Therefore, a pressure gradient model can only be applied after the definition of which flow pattern behaves as segregated or dispersed flow. The pressure gradient data are compared with predictions of the two-fluid model for segregated flow and the homogeneous model for dispersed flow.

## 4. Results and discussion

### 4.1. Flow regimes

The flow regimes were determined based on visual observations and local water volume fraction measurements. A high speed camera and a still picture camera were used to visualize the flow. The oil-water flow patterns observed in the present work are in line with the flow pattern classifications proposed by Trallero et al. (1997), Rodriguez et al. (2006) and Lum et al. (2006). The investigated flow cases were categorized into different flow regimes as given in the table 2.

**Table 2.** Observed flow regimes.

Flow regime	Abbreviation
Segregated flow	
Stratified smooth	ST
Stratified wavy	SW
Stratified flow with mixing at the interface	ST&MI
Dispersed flow	
Water dominated	
Dispersion of oil-in-water and water	Do/w&w
Oil-in-water dispersion	Do/w
Oil dominated	
Dispersion of oil-in-water and water-in-oil	Do/w&w/o
Water-in-oil dispersion	Dw/o
Plug flow	PF

#### 4.1.1. Segregated flow

For low superficial oil and water velocities the flow is gravity dominated and the phases are segregated. Apparently, at low superficial velocities the dispersive turbulent forces are not large enough to induce interfacial waves and droplet entrainments. The oil-water interface was smooth and stable. Figure 6(a) illustrates typical stratified smooth (ST) oil-water flow where  $U_m=0.25$  m/s,  $\lambda_w=0.25$  and  $\xi=0^\circ$ . A further increase in the flow rates causes the appearance of interfacial waves. There are capillary waves, probably modified by the shear stress caused by the presence of the pipe wall. The flow regime is called stratified wavy (SW) flow and shown in figure 6(b) where  $U_m=0.25$  m/s,  $\lambda_w=0.50$  and  $\xi=+5^\circ$ . The stratified wavy flow pattern is specially observed in upwardly inclined flow. The most important hydrodynamic feature of this flow pattern is the stable wavy structure of the interface. It is not observed any sign of mixing at the interface. Along the interfacial waves at higher velocities, water droplets exist in the oil layer and oil droplets in the water layer. This flow pattern is named as stratified flow with mixing at the interface (ST&MI). Figure 6(c) depicts this flow regime where  $U_m=0.50$  m/s,  $\lambda_w=0.25$  and  $\xi=0^\circ$ . Dynamic and buoyant forces act simultaneously on the droplets. The dynamic forces that tend to spread the droplets throughout the pipe cross section are not large enough to overcome the settling tendency of the counteracting gravity forces. Hence, both kinds of droplets remain close to the interface. The mechanism of droplet formation was not obvious. Guzhov et al. (1973) observed that the relative movement of the phases results in the development of vortex motion at the boundary of the two liquids. The mutual penetration of vortices takes place in each of the phases. This interface turbulence leads to the dispersion of liquids.

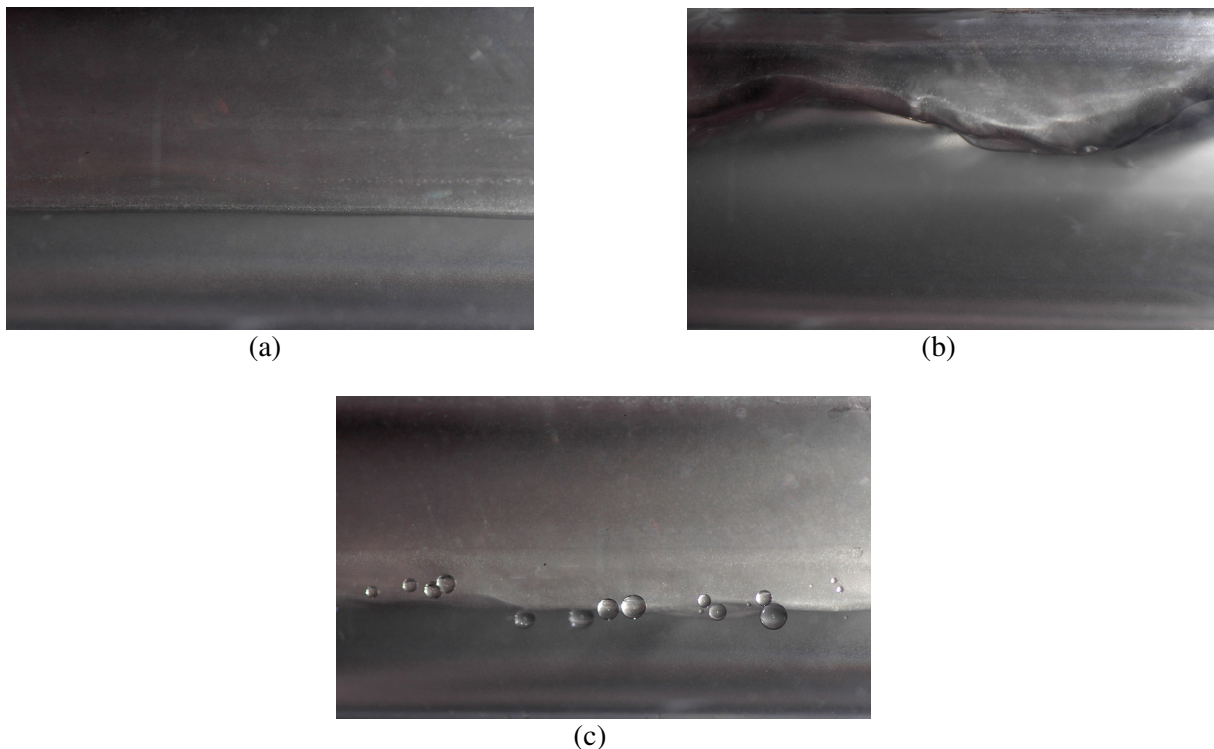


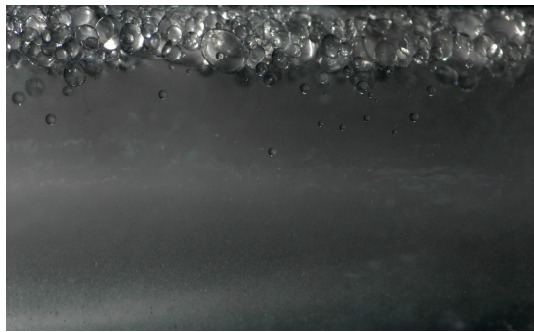
**Figure 6.** Segregated oil-water flow: (a) Stratified smooth (ST), (b) Stratified wavy (SW), (c) Stratified flow with mixing at the interface (ST&MI).

#### 4.1.2. Dispersed flow

Outside the stratified region, the flow patterns are different dispersions. Dispersions are always formed when the motion of oil-water flow is sufficiently intense. For larger water superficial velocities the flow is water dominated. Water vortices appearing at the interface enter into the oil layer and tend to

disperse it. The water could remain as a continuous layer while oil loses its continuity and moves as discrete pieces separated by water. When the water superficial velocity is further increased, the frequency and intensity of water vortices increase, and more and smaller discrete pieces are formed. The dispersive turbulent energy in the water phase is not sufficient to distribute oil droplets over the entire cross section of the pipe. Then, the upward buoyancy prevails, and a dispersion of oil-in-water is formed over the water layer. However, the water layer may have small oil entrainment. This flow pattern is illustrated in figure 7(a) where  $U_m=0.50$  m/s,  $\lambda_w=0.95$  and  $\xi=+5^\circ$ . At higher water superficial velocities the oil phase is completely dispersed and oil appears in the form of droplets in a water continuous matrix. The turbulent forces are sufficient to maintain a homogeneous dispersion over the cross section of the pipe. The flow pattern is called as oil-in-water dispersed flow (Do/w) and illustrated in figure 7(b) where  $U_m=2.50$  m/s,  $\lambda_w=0.90$  and  $\xi=+5^\circ$ .

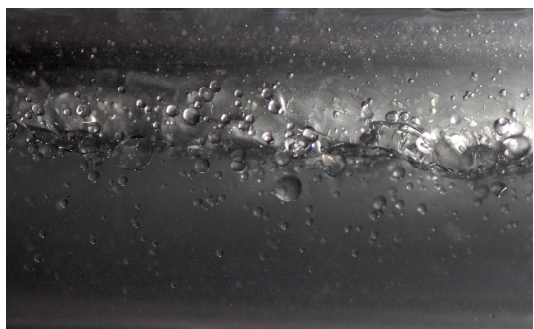
On the other hand, oil is the dominant phase for small water fractions. The interfacial mixing region grows with an increase in velocity and the two types of dispersions coexist. In this case both phases retain their continuity at the top and the bottom of the pipe but with each phase dispersed, at various degrees, into the continuum of the other. The flow regime is defined as dispersion of oil-in-water and water-in-oil flow (Do/w&w/o) as shown in figure 7(c). The flow conditions are maintained at  $U_m=1.00$  m/s,  $\lambda_w=0.50$  and  $\xi=+5^\circ$ . The same flow pattern was defined as dual continuous flow by Lovick et al. (2004). Water-in-oil (Dw/o) dispersed flow is created at higher oil superficial velocities together with small inlet water volume fractions. Here, again dispersive turbulent forces are large enough to prevent sedimentation and coalescence of water droplets into a continuous water layer. At relatively high oil superficial velocities water is homogeneously dispersed in the oil phase. The flow pattern is illustrated in figure 7(d) where  $U_m=1.50$  m/s,  $\lambda_w=0.025$  and  $\xi=+5^\circ$ .



(a)



(b)



(c)



(d)

**Figure 7.** Dispersed oil-water flow: (a) Dispersion of oil-in-water and water (Do/w&w), (b) Dispersion of oil-in-water (Do/w), (c) Dispersion of oil-in-water and water-in-oil (Do/w&w/o), (d) Dispersion of water-in-oil (Dw/o).

The plug flow (PF) regime occurs at pipe inclination  $+5^\circ$ , for mixture velocity 0.25 m/s, and for inlet water cuts above 0.925. This flow pattern is characterized by a thick plug of oil flowing at the top of the pipe. The sizes of the plugs are not uniform. Flores et al. (1998) has called these oil plugs as pseudoslugs. These plugs become gradually thinner until it is replaced by either oil droplets or virtually single-phase water. The oil plug then re-appears, reinstating the oil-water mixture. The sequence of events of plug flow is shown in figure 8 with  $U_m=0.25$  m/s,  $\lambda_w=0.95$  and  $\xi=+5^\circ$ .

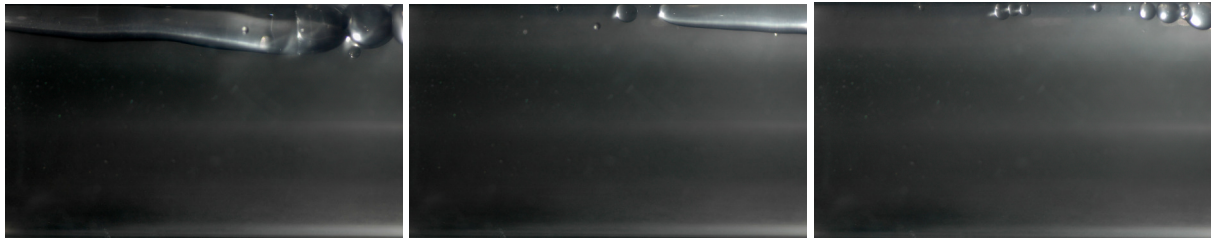


**Figure 8.** Plug flow at pipe inclination  $+5^\circ$ ,  $U_m=0.25$  m/s and  $\lambda_w=0.95$ .

#### 4.1.3. Flow pattern maps

The flow patterns of oil-water flow in horizontal and slightly inclined pipes are presented in terms of flow pattern maps for different mixture velocities and inlet water cuts. Figure 9 shows the flow pattern map for horizontal oil-water flow. Stratified smooth flow pattern is observed for intermediate water cuts ( $0.075 < \lambda_w < 0.90$ ) at mixture velocity 0.25 m/s. At lower and higher water cuts ST&MI flow pattern is observed. As the mixture velocity increases to 0.50 m/s, ST flow regime observed at low mixture velocity is replaced by ST&MI flow pattern. Do/w&w flow regime is observed for higher water cuts ( $\lambda_w > 0.875$ ) at mixture velocity 0.50 m/s. The dual continuous flow regime is observed at mixture velocity 0.75 m/s, for inlet water cuts upto 0.85. Do/w&w flow regime is observed at lower inlet water cuts at mixture velocity 0.75 m/s compared to 0.50 m/s. At mixture velocity 1.00 m/s and inlet water cut 0.025, water is completely dispersed in the oil and Dw/o flow pattern is observed. At higher water cuts oil is completely dispersed in the water and Do/w flow is observed above the inlet water cut 0.95. As the mixture velocity increases, Dw/o flow regime extends to the higher water cuts and the region in which Do/w&w/o flow occurs is strongly reduced while regions with Dw/o and Do/w flow increase in size.

Figure 10 shows the flow pattern map at pipe inclination  $+1^\circ$ . Stratified smooth flow observed at mixture velocity 0.25 m/s for horizontal flow is completely replaced by ST&MI flow. A comparison of flow pattern maps between upwardly inclined at  $+1^\circ$  and horizontal flow shows that the level of dispersion in the former is greater for the same flow conditions. In addition, the Dw/o flow regime shrinks towards lower inlet water cuts while Do/w&w and Do/w flow regimes are expanded towards lower water cuts. These shifts in dispersed flow regime boundaries are attributed to the increased in situ water volume fraction with upward inclination, which encourages the development of water-dominated flow patterns and delays the onset of oil-dominated ones.

In the  $+5^\circ$  inclined flow, significant changes in the flow pattern map are observed due to two new flow patterns, stratified wavy (SW) and plug flow (PF) as shown in figure 11. Stratified wavy flow pattern is observed at mixture velocity 0.25 m/s for inlet water cuts from 0.25 to 0.90. The plug flows (PF) are observed at higher inlet water cuts ( $\lambda_w > 0.90$ ) at mixture velocity 0.25 m/s. The Dw/o flow pattern further shrinks in terms of inlet water cuts, but not with mixture velocity. An expansion of Do/w flow regime is observed. At higher mixture velocities, the pipe inclination has negligible influence for the transition from Do/w to Do/w&w and from Do/w&w to Do/w&w/o.

The flow pattern map at pipe inclination  $-1^\circ$  is given in figure 12. Stratified smooth flow pattern is observed for inlet water cuts from 0.20 to 0.60. At  $-1^\circ$  the Do/w flow regime is observed at lower mixture velocities for higher inlet water cuts compared to the horizontal and upwardly inclined flows.

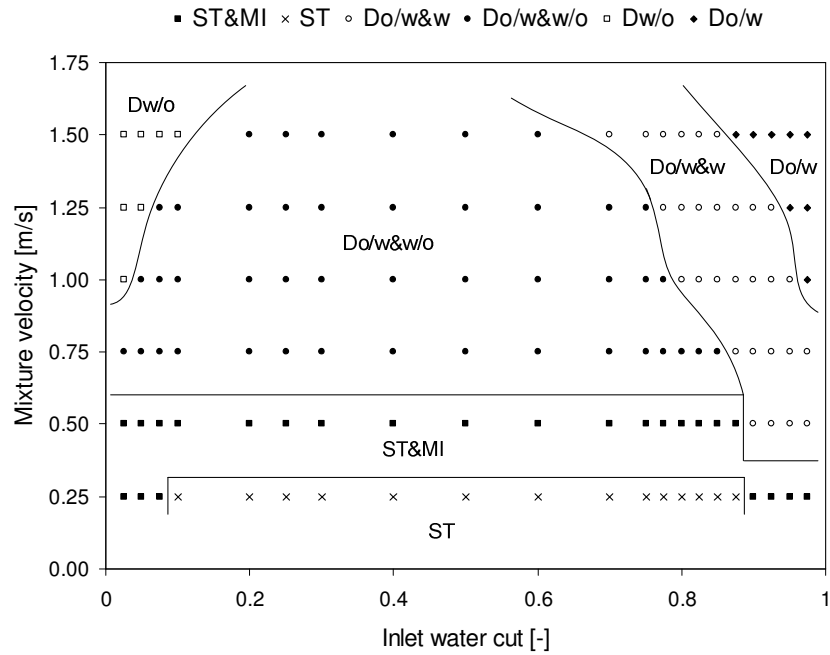


**Figure 9.** Flow pattern at pipe inclination  $0^\circ$ .

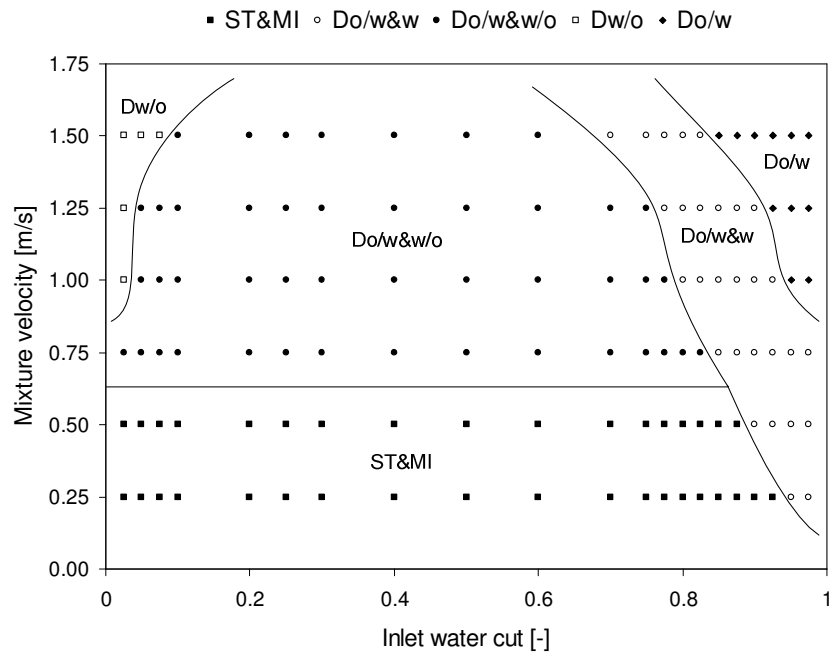


**Figure 10.** Flow pattern map at pipe inclination  $+1^\circ$ .

The higher velocity of the water layer at pipe inclination  $-1^\circ$  increases the amount of oil dispersed in water and makes the transition from Do/w&w to Do/w to appear at lower mixture velocities. Figure 13 depicts the observed flow patterns at pipe inclination  $-5^\circ$ . Stratified smooth flow observed at mixture velocity 0.25 m/s is replaced by ST&MI flow. The Dw/o flow regime observed at low water cuts is further extended to higher water cuts. The Do/w&w flow regime is observed at higher inlet water cuts at lower mixture velocities in contrast with ST&MI flow regime observed at pipe inclination  $-1^\circ$ . In addition, Do/w flow regime is also expanded towards lower water cuts. These observations can be directly related to the increased in situ water velocities at pipe inclination  $-5^\circ$ .

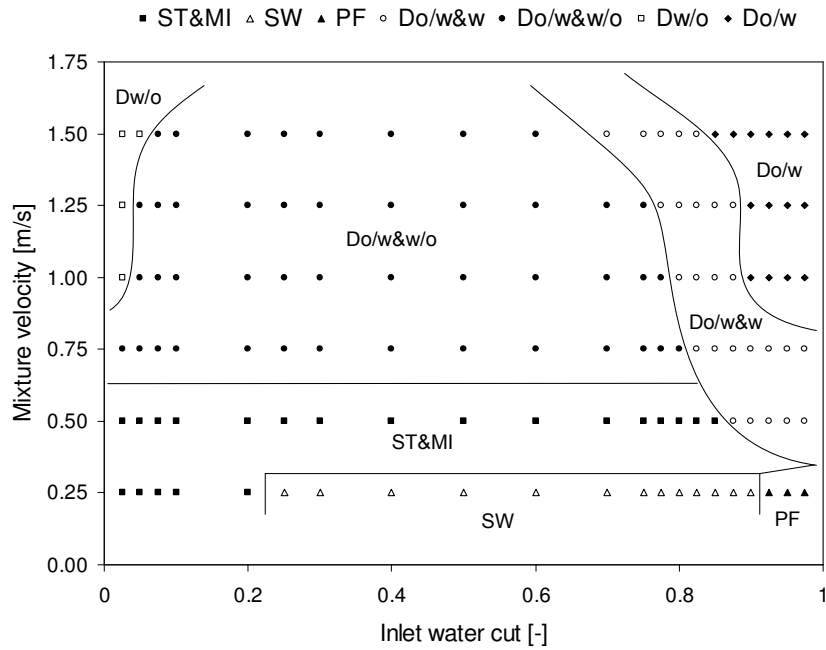


**Figure 11.** Flow pattern map at pipe inclination +5°.

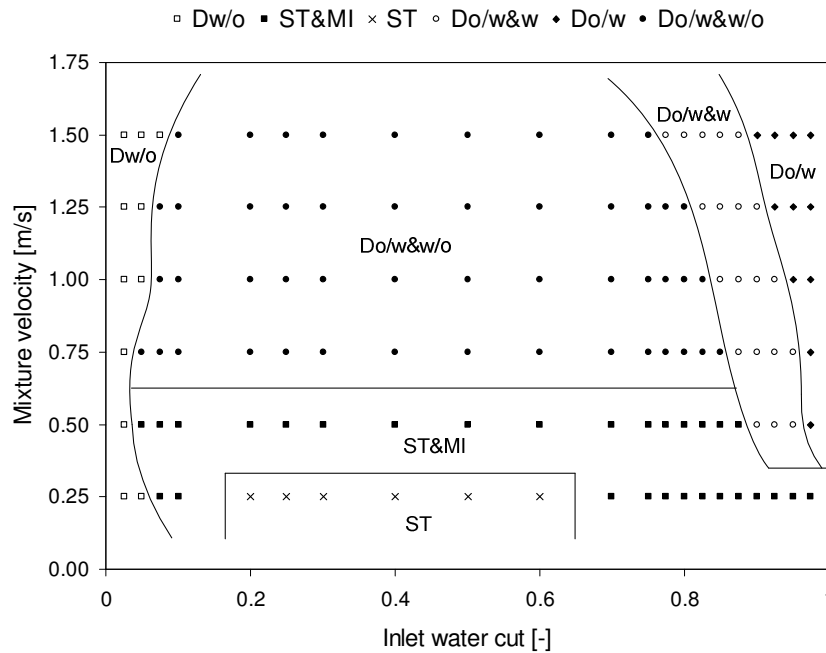


**Figure 12.** Flow pattern map at pipe inclination -1°.

In comparing the current results with those of previous investigations there is an acceptable consensus on the flow behaviour at this range of flow conditions. A general agreement exists that in inclined flows dispersion appears at lower velocities than in the horizontal flows (Oddie et al., 2003; Lum et al., 2004). Lum et al. (2006) and Rodriguez et al. (2006) reported SW flow regime in upwardly inclined flows which replace ST flow regime observed in horizontal flows for the same flow conditions. Similar flow behaviour is observed in the present study. The time dependent plug flow regime observed in the present work is similar to the results obtained by Lum et al., (2006). The slight decrease of the Dw/o regime in the current work with increased inclination is in good agreement with

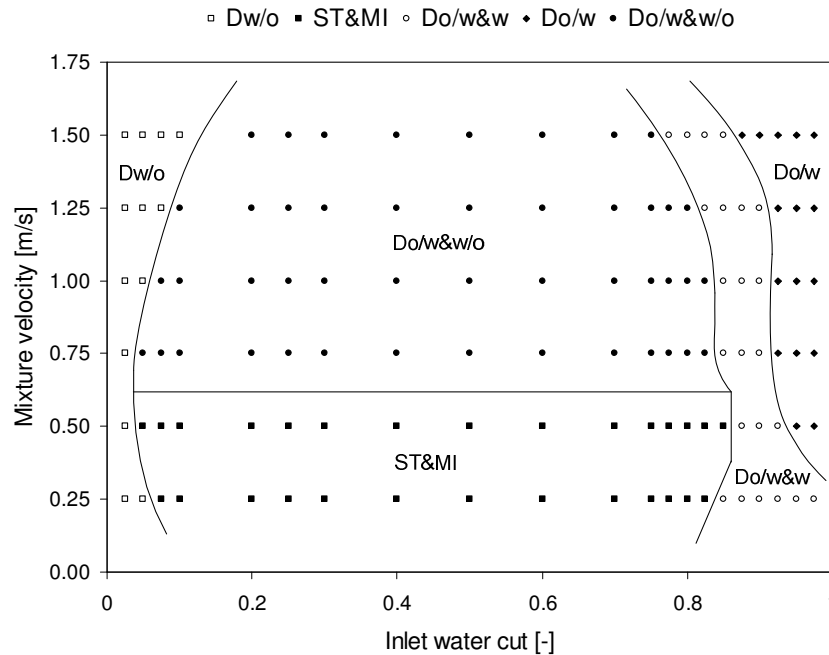


**Figure 13.** Flow pattern map at pipe inclination  $-5^\circ$ .

the results presented by Lum et al. (2006). The range of the dispersed oil-in-water (Do/w) flow regime increases as the inclination is increased (Lum et al., 2006). This is related to the in situ water content associated with increased upward inclination. Similar behaviour of the Do/w flow regime is observed in the present work. Cox (1985) and Alkaya (2000) observed that the transition from separated to dispersed flow occurs at lower velocities in downwardly inclined flows than in horizontal flow. In contrast to the current work stratified wavy flow pattern has been observed in downwardly inclined flows by other investigators (Cox, 1985; Alkaya, 2000; Oddie et al., 2003; Abduvayt et al., 2004; Rodriguez et al., 2006). This could be due to the different ranges of velocities, fluid properties and pipe geometries used in their experiments. The plug flow regime is not observed in the downwardly inclined flow and this is in accordance with previous work done by Cox (1985), Alkaya (2000), Oddie et al. (2003), Abduvayt et al. (2004) and Lum et al. (2006). An extensive level of increase in Do/w flow regime has been observed in downwardly inclined flows by Lum et al. (2006), in accordance with the present observations. According to Alkaya (2000), downward inclination slightly enhanced the dispersed water-in-oil flow pattern so that it appears at lower mixture velocities at pipe inclination  $-5^\circ$ , but not at  $-1^\circ$ . However, in the present work Dw/o flow regime is observed at lower inlet water cuts for pipe inclinations  $-1^\circ$  and  $-5^\circ$ .

#### 4.2. Local water volume fraction measurements

Gamma densitometry is an accurate, but slow measurement technique. It can only measure time averaged hold-ups and will not be able to capture transient effects like wave structure of the flow. By traversing horizontal gamma beams the time averaged water volume fraction is measured as a function of vertical pipe position. Figure 14(a) shows typical raw data from the gamma densitometer. It shows the single-phase calibration curves together with two-phase oil-water flow measurements for stratified and dispersed flows. The number of counts (or intensity) received is plotted on the y-axis of the graph and the linear (vertical) position of the pipe is plotted on the x-axis. Since the densities before entering into the inside of the pipe are equal at the bottom and at the top of the pipe section (provided there is a constant pipe thickness), the intensity should be equal as shown in figure 14(a). Therefore the inner pipe wall extends from 3 mm to 59 mm. The stratified flow measurements shown in figure 14(a) follows the intensity measurements for pure water upto 17 mm and it follows intensity measurements

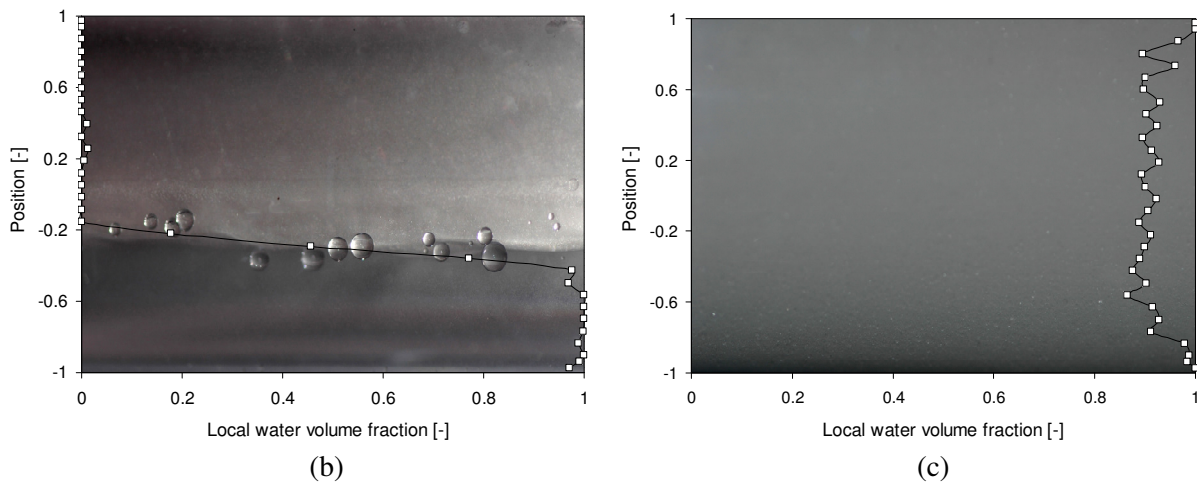
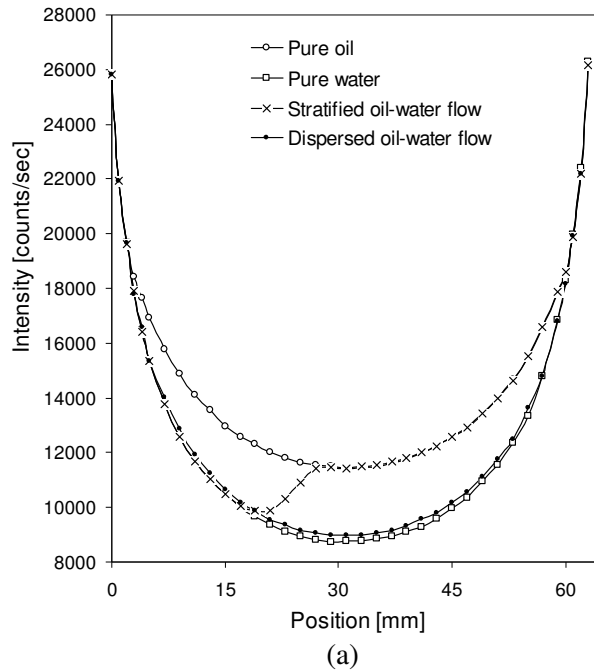


**Figure 14.** Local water volume fraction measurements: (a) Raw gamma densitometry data, (b) Stratified oil-water flow, (c) Dispersed oil-water flow.

for oil from 28 mm. The intensity varies from pure water to pure oil across the interface. Therefore the flow regime is stratified flow and it is confirmed by visual observations given in figure 14(b). By using equation 3 the raw intensity data can be converted into local water volume fractions. Figure 14(b) shows the local water volume fraction measurements when the flow conditions are  $U_m=0.50$  m/s,  $\lambda_w=0.25$  and  $\xi=0^\circ$ . The direction of the flow is from left to right with the oil phase in the upper part of the pipe. The local water volume fraction is expected to be zero in the oil phase and one in the water phase. At the interface it will be somewhere in between. Good agreement between measurements and visual observations can be seen except for the measurement points close to the wall in the water phase. While measuring close to the pipe wall, parts of the gamma beams hit the wall instead of the flow, making the control volume very small. The accuracy of the gamma densitometer decreases with decreasing control volume, and severely reduced accuracy is expected in the measurements closest to the pipe wall. For the dispersed oil-water flows the measured intensity is somewhere in



between pure water and pure oil throughout the pipe cross-section as shown in figure 14(a). The flow conditions are maintained at  $U_m=2.50$  m/s,  $\lambda_w=0.90$  and  $\xi=+5^\circ$ . Figure 14(c) shows the corresponding water volume fraction measurements. In this case the oil phase is homogeneously dispersed in the water.

#### 4.2.1. Effects of changes of mixture velocity

In figure 15 a comparison of local water volume fraction measurements for different mixture velocities and inlet water cuts is given for horizontal oil-water flow. Figure 15(a) shows local water volume fraction measurements for three different inlet water cuts (0.25, 0.50 and 0.75) at mixture velocity 0.50 m/s. The figure shows that increasing inlet water cut gives increasing water hold-up. Here oil and water phases are separated by a sharp interface for the given water cuts. Therefore the given flow conditions make segregated oil-water flows. At inlet water cut 0.50, the mixing at the interface is low compared to the flow at inlet water cut 0.25 and 0.75. Therefore the thickness of the interface region is lower at the inlet water cut 0.50 compared to the inlet water cut 0.25 and 0.75.

Figure 15(b) shows gamma measurements for three different inlet water cuts at mixture velocity 1.50 m/s. As seen in the picture, the interface region is thicker than segregated flow cases given in figure 15(a). This is due to the waves and the entrained droplets around the interface. According to figure 15(b), most of the water is dispersed in oil when the inlet water cut is 0.25. A thick interface region is observed together with pure oil layer in the upper part of the pipe. When the inlet water cut is increased to 0.50, a continuous water layer is formed. Oil phase is completely dispersed in the water phase at the inlet water cut 0.75.

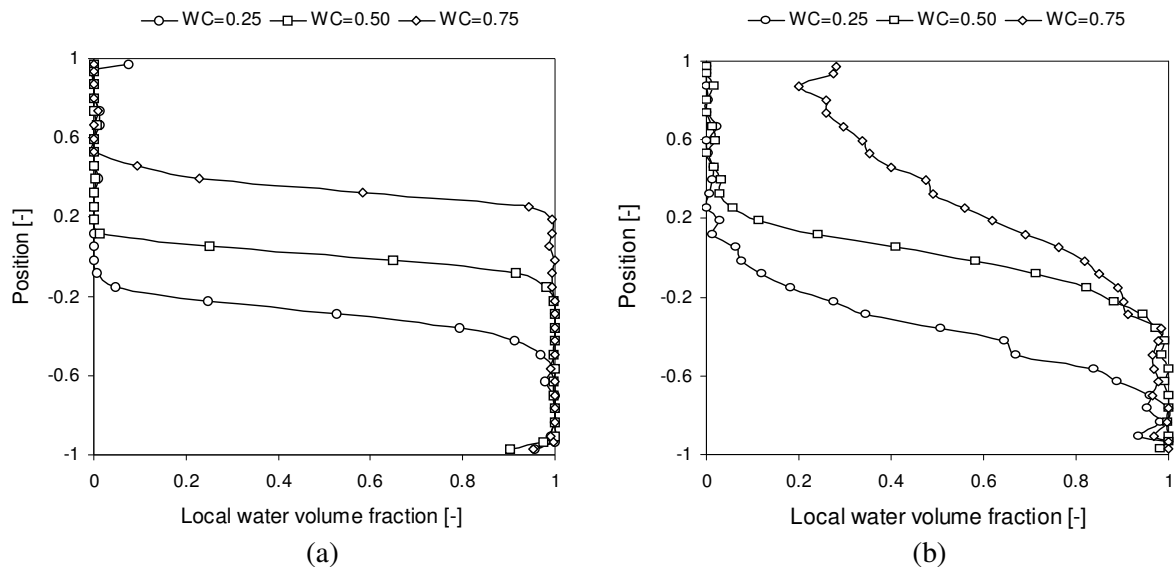


**Figure 15.** Comparison of gamma measurements for different mixture velocities and inlet water cuts for horizontal flow: (a) Mixture velocity = 0.50 m/s, (b) Mixture velocity = 1.50 m/s.

#### 4.2.2. Effects of changes of pipe inclination at mixture velocity 0.25 m/s and inlet water cut 0.50

Figure 16 depicts local water volume fraction measurements for different pipe inclinations at mixture velocity 0.25 m/s and inlet water cut 0.50. In horizontal flows, at low mixture velocities, a sharp change in the water volume fraction is observed across the interface. As shown in figure 16(a) the water hold-up increases when the pipe inclination is increased upwardly. The stratified wavy flow is observed with large amplitude interfacial waves at pipe inclination  $+5^\circ$ . Hence, sharp interface

between the two phases is absent compared to the corresponding flow conditions at pipe inclination  $0^\circ$  and  $+1^\circ$ .

Figure 16(b) shows a comparison of local water volume fraction measurements for downwardly inclined flows at various pipe inclinations. The flow conditions are maintained at  $U_m=0.25$  m/s and  $\lambda_w=0.50$ . The water hold-up decreases when the pipe is downwardly inclined. A thick interface region is observed at pipe inclination  $-5^\circ$  due to the increased mixing around the interface.

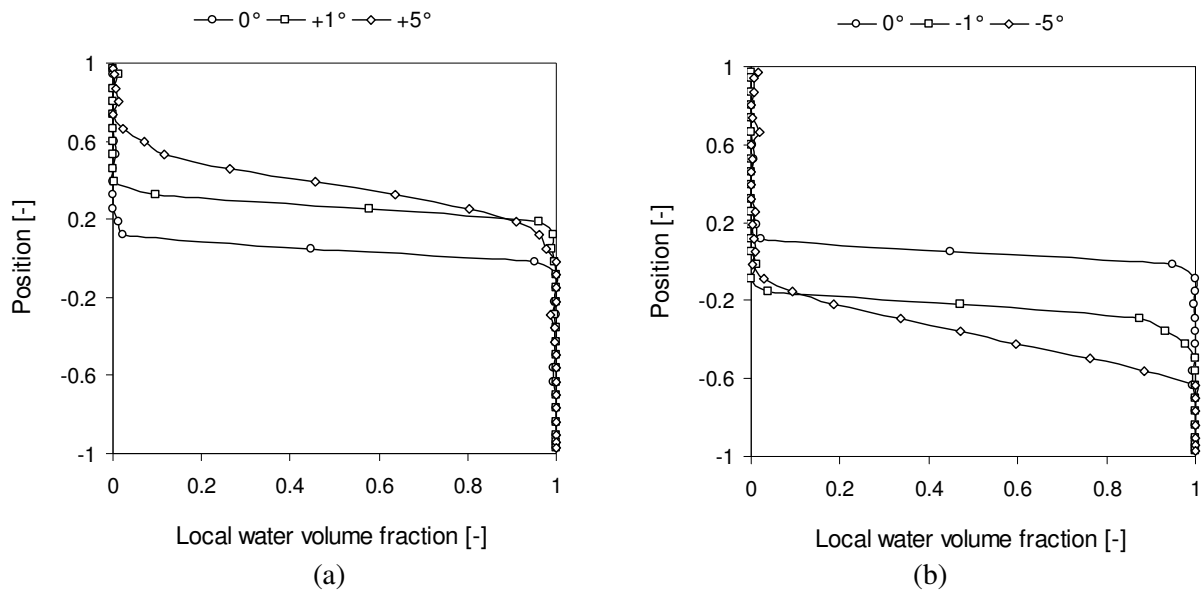


**Figure 16.** Comparison of gamma measurements for different pipe inclinations ( $U_m=0.25$  m/s and  $\lambda_w=0.50$ ): (a) Upward flow, (b) Downward flow.

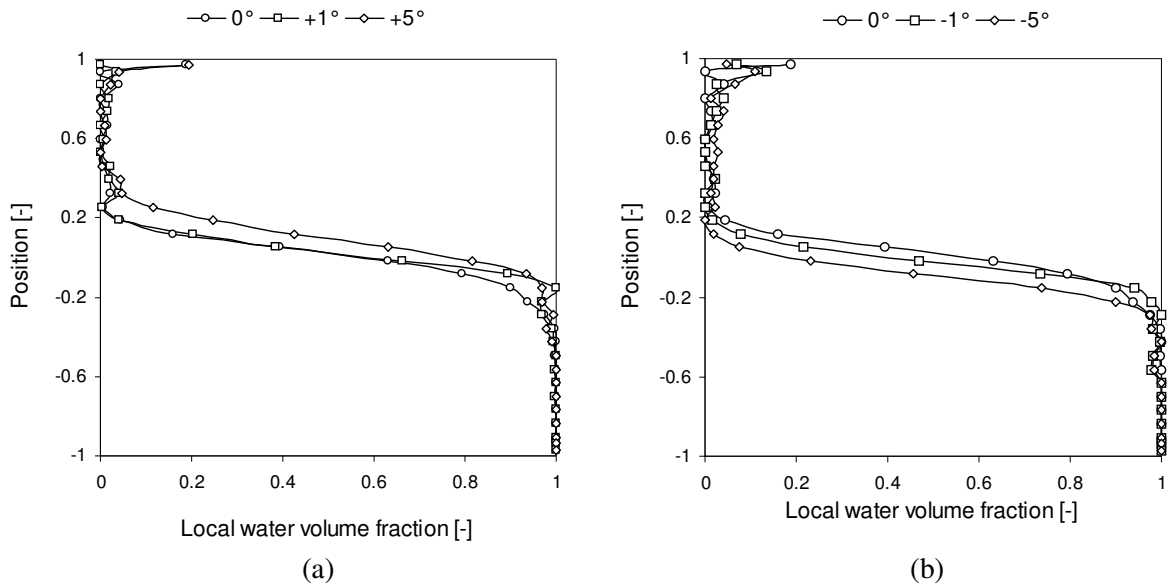
#### 4.2.3. Effects of changes of pipe inclination at mixture velocity 1.00 m/s and inlet water cut 0.50

In figure 17 gamma densitometry measurements of different inclination angles are compared for oil-water flows with mixture velocity 1.00 m/s and inlet water cut 0.50. In general, water hold-up increases as the pipe inclination increases upwardly. However, the differences between local water volume fraction measurements for horizontal and upwardly inclined flows are very small compared to the results at low mixture velocity,  $U_m=0.25$  m/s. In this case, the effects of gravitational forces are moderated by increased flow momentum.

Figure 17(b) shows local water volume fraction measurements for downwardly inclined pipes at  $U_m=1.00$  m/s and  $\lambda_w=0.50$ . The water hold-up decreases when the pipe is downwardly inclined as expected. The difference between the local water volume fraction measurements for horizontal and downwardly inclined ( $-1^\circ$ ) flow is distinct compared to upwardly inclined ( $+1^\circ$ ) flows as shown in figure 17(a). In general, the gamma measurements at higher mixture velocities show less variations compared to the results at lower mixture velocities.

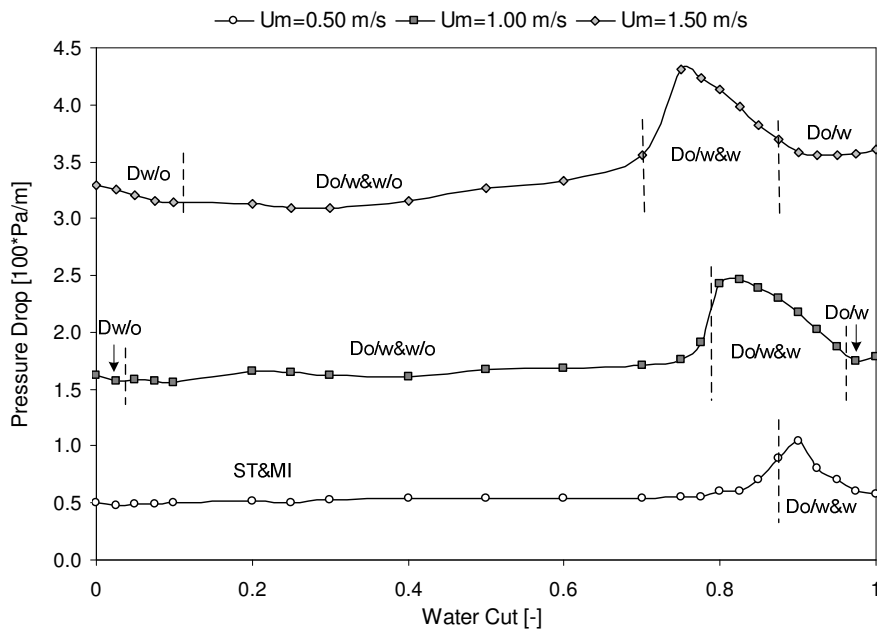
#### 4.3. Pressure drop measurements

Figure 18 shows the measured pressure gradient as a function of the inlet water cut for three different mixture velocities ( $U_m=0.50$  m/s,  $U_m=1.00$  m/s and  $U_m=1.50$  m/s) for horizontal oil-water flows. The identified flow patterns are indicated close to the reported pressure drop data. The measured pressure drop shows significant variations from single-phase oil to single-phase water. One rather striking feature of pressure drop in oil-water flow is observed at higher water cuts. The pressure drop increases quite dramatically at higher water cuts where Do/w&w flow pattern is observed. In Do/w&w flows, all the oil is dispersed in water and flows over the pure water layer. The increase in the measured pressure gradient is the result of an increased effective (or emulsion) viscosity resulting from interaction of the



**Figure 17.** Comparison of gamma measurements for different pipe inclinations ( $U_m=1.00$  m/s and  $\lambda_w=0.50$ ): (a) Upward flow, (b) Downward flow.

dispersed droplets. The peak in pressure drop is observed at about inlet water cut 0.90 for mixture velocity 0.50 m/s and shifts towards lower water cuts as the mixture velocity increases. At 1.00 m/s and 1.50 m/s the peak is observed at inlet water cut 0.81 and 0.76, respectively. At higher mixture velocities oil phase is dispersed in water phase at lower water cut compared to low mixture velocities. Therefore the peak in pressure drop is observed at lower water cut for high mixture velocities compared to low mixture velocities. The investigation by Nädler et al. (1997) indicate that phase inversion takes place within the dispersion layer and hence only in a restricted area of the pipe. The higher frictional pressure drop values that they observed at higher inlet water cuts have been attributed



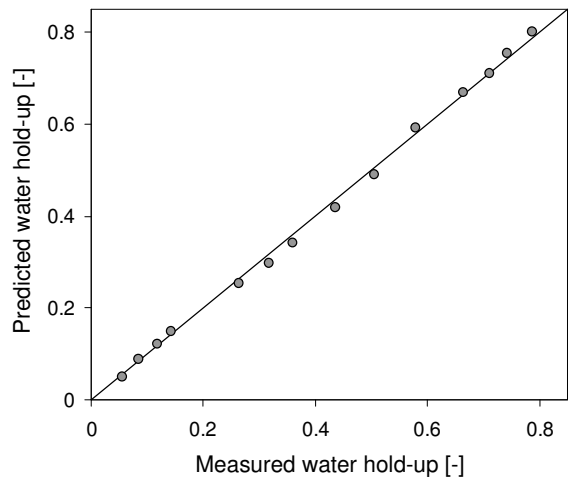
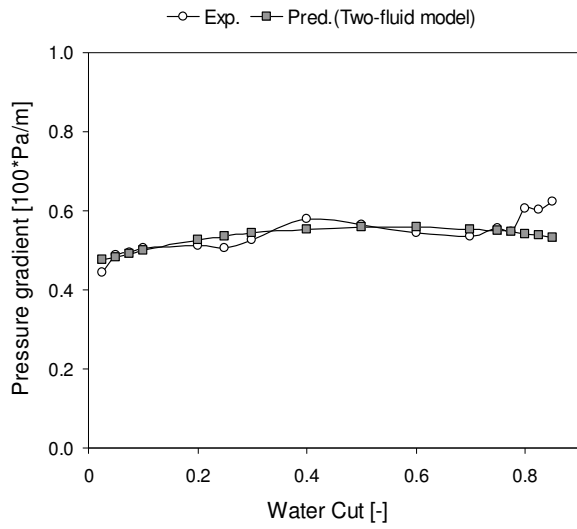
**Figure 18.** Comparison of pressure drop measurements at different mixture velocities for horizontal oil-water flow.

to the partial inversion effect. Elseth (2001) has also reported similar behavior of the frictional pressure drop of oil-water flow in horizontal pipes in comparison with present results. A peak in pressure drop around the point of inversion (approximately at water cut 0.40) as observed by several investigators (Valle et al., 1997; Angeli et al., 1998) is not seen in any of the experiments. Most likely the mixture velocity is too small for expected peak to appear. Also, the mixing unit (see figure 2) at the entrance of the test section is designed in a way that reduces dispersions. As shown in figure 18 the pressure drop is slightly decreased at low water cuts when the inlet water cut is increased at high mixture velocities ( $U_m=1.50$  m/s). Soleimani et al. (1997) and Soleimani (1999) also reported a similar fall in pressure drop at low water cuts. The phenomenon is probably attributed to the formation of oil continuous dispersions. According to Soleimani (1999), the presence of drops will repress turbulence making a drag reduction effect which reduces the pressure gradient. At low mixture velocities ( $U_m=0.50$  m/s) the flow is stratified even at low water cuts, and therefore no initial fall in pressure drop is observed.

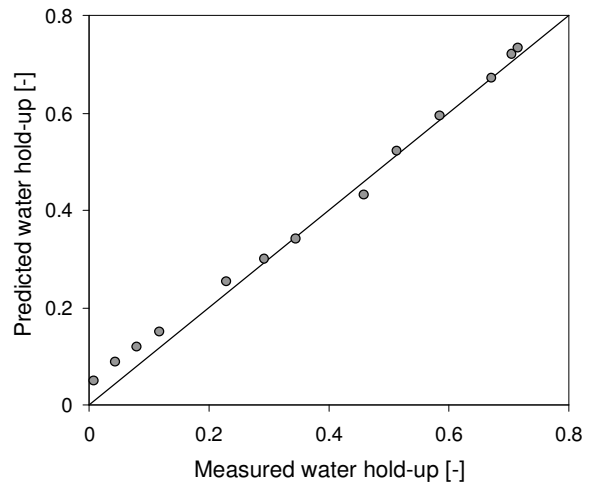
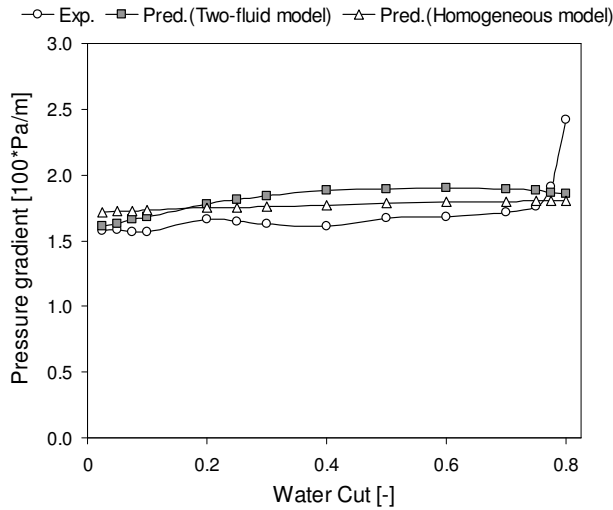
#### 4.4. Experimental results and model comparisons

Figure 19(a) shows the comparison of predicted and measured pressure drop and water hold-up results for segregated oil-water flow in horizontal pipes at mixture velocity 0.50 m/s. The experimental results are compared with model predictions based on the two-fluid model. The agreement is quite acceptable except at higher input water cuts ( $\lambda_w > 0.775$ ). When the inlet water cut is below 0.775, the flow is classified as segregated flow and ST&MI flow regime is observed with weak interface mixing between two phases. A thin interface region is also observed as shown in figure 15(a). Therefore the assumptions behind the two-fluid model are acceptable under these flow conditions and it gives better predictions. At high inlet water cuts, oil is dispersed in water and densely packed layer of oil droplets is formed and flows over the water phase. The pressure drop increases as a result of this dispersion effect. The flow regime is categorized as dispersion of oil-in-water and water flow. These flow conditions are difficult to model with two-fluid model based on segregated flow. Therefore the predicted pressure drops deviate significantly from the experimental data at higher water cuts. Elseth (2001) and Rodriguez et al. (2006) observed that in general the pressure drop data fit the two-fluid model best for intermediate water cuts, whereas for higher water cuts the model under-predicts the pressure drop. Similar trend is observed in the present work. The experimental water hold-up values are calculated based on gamma measurements. The vertical distance from the bottom of the pipe to the point where the local water volume fraction is equal to 0.50 is considered as the interface height in order to calculate the flow areas occupied by oil and water. The interface is treated as a flat surface. The predicted water hold-up values were calculated based on the two-fluid model. As shown in figure 19(a) the agreement between measured and predicted water hold-ups is seen to be quite reasonable.

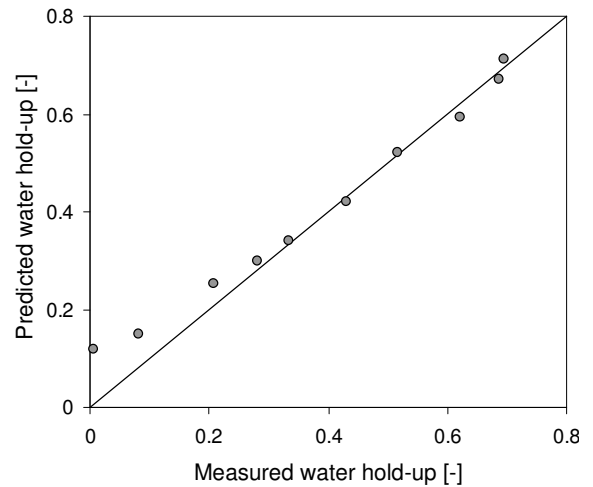
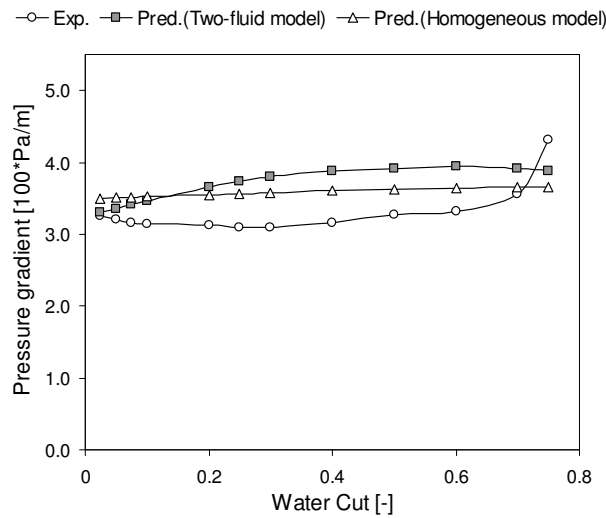
The hold-up predictions depend on the flow-pattern. Hence, the choice for a suitable hold-up model can only be made after the definition of which flow pattern behaves as stratified or dispersed flow. Unfortunately, the choice is not trivial, especially for the case of dual-continuous flows. Dual-continuous flows are somewhat between the stratified and fully-dispersed flows in terms of the in situ distribution of the phases (Lovick et al., 2004). Dual-continuous flow are observed at higher mixture velocities,  $U_m$  (1.00 and 1.50 m/s), for intermediate water cuts as shown in figure 9. Therefore, the experimental results are compared with model predictions based on both two-fluid and homogeneous models. The prediction accuracies of different models are discussed for dual-continuous flows. Figure 19(b) shows a comparison of model predictions and experimental measurements of frictional pressure drop and water hold-up at mixture velocity 1.00 m/s. The measured pressure drop is compared with model predictions based on both two-fluid and homogenous models. The two-fluid model over-predicts the pressure drop at intermediate water cuts where dual continuous flow regime is observed. Valle et al. (1995) have compared two-fluid model against data for Exxsol D80 oil-water mixtures. They states that the two-fluid model overestimates the pressure drop data and the over-prediction increases as mixture velocity increases. The main reason behind this over-prediction is probably due to dispersed drops entrained in the respective oil and water continuous zones that coalesce with each



(a)



(b)



(c)

**Figure 19.** Comparison of predicted and experimental results for oil-water flow in horizontal pipe: (a)  $U_m=0.50$  m/s, (b)  $U_m=1.00$  m/s, (c)  $U_m=1.50$  m/s.

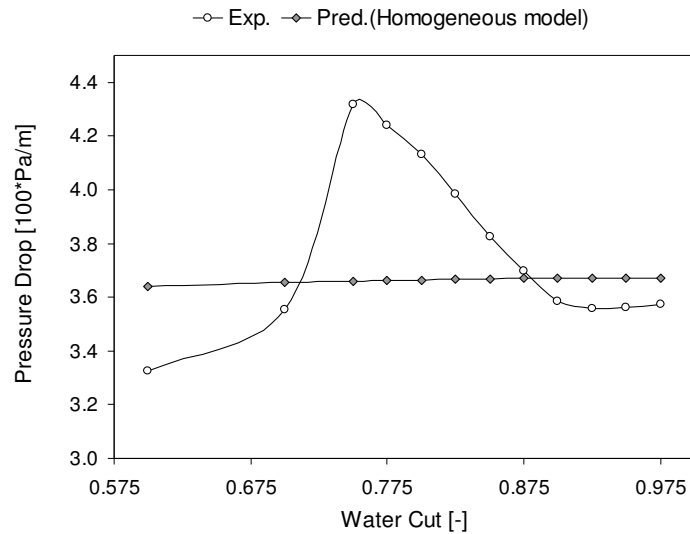
other and with the oil-water interface (Valle, 1998). Hence, the dispersions are unstable and a drag reduction effect can be expected particularly in the oil-continuous dispersions (Pal, 1993; Hardin, 1995). The two-fluid model severely under-predicts the pressure drop at inlet water cut 0.80 where the transition from Do/w&w/o to Do/w&w flow is occurred. This indicates that the standard two-fluid model is not able to predict the Do/w&w flow regime. The maximum deviation of 23% between two-fluid model predictions and measured data is observed at inlet water cut 0.80 and the absolute error of the predictions is about 6%. Even though, the Do/w&w/o flow pattern presents features of both stratified and dispersed flows, the homogeneous model gives slightly better predictions of measured pressure gradients compared to the two-fluid model. However, the homogeneous model over-predicts the pressure drop with an absolute error of 4%. In the Dw/o flow region at lower inlet water cuts the homogenous model slightly overestimates the pressure gradient data. Rodriguez et al. (2006) have reported similar results using homogeneous model in modelling oil-water flows. As can be seen in figure 19(b), a good agreement between predicted and measured water hold-ups is observed. The predicted water hold-up values are estimated based on two-fluid model. However, the model over-predicts the water hold-up data at lower water cuts. At the lower water cuts the water phase tends to disperse in the oil phase and loses its continuity. Hence, the hold-up predictions based on two-fluid model that assumes stratified oil and water phases can be deviated from measured values at lower water cuts. At intermediate water cuts the model gives better results.

Figure 19(c) shows a comparison of model predictions and measurements of pressure drop and water hold-up at mixture velocity 1.50 m/s. The two-fluid model over-predicts the pressure drop of dual continuous flow at intermediate water cuts. The over prediction has increased as a result of increased mixture velocity, in accordance with previous investigations by Valle et al. (1995). This can be directly attributed to the increased level of mixing between oil and water phases at higher mixture velocities. The maximum deviation of 23% between two-fluid model predictions and measured data is observed at inlet water cut 0.40 and the absolute error of the predictions is about 12%. The homogeneous model gives better predictions of pressure gradient compared to the two-fluid model for dual continuous flow. However, the homogeneous model overestimates the pressure gradient with an absolute error of 9%. The model over-predicts pressure gradient data in the Dw/o flow regime at lower water cuts. Both models show severe deviations at the boundary where the transition from Do/w&w/o to Do/w&w flow is occurred around inlet water cut 0.75. Lovick et al. (2004) stated that the standard two-fluid is unable to predict the pressure gradient during dual-continuous flow. The conclusion is further confirmed with the present results. The water hold-up predictions based on two-fluid model, deviates significantly from the measured data at lower and higher water cuts. However, the model gives acceptable predictions at intermediate water cuts ( $0.25 < \lambda_w < 0.60$ ) as shown in figure 19(c).

Figure 20 shows a comparison between predicted and measured pressure drop results at mixture velocity,  $U_m = 1.50$  m/s. The results are presented only at higher water cuts where Do/w&w and Do/w flows are observed ( $\lambda_w > 0.70$ ). The model gives acceptable results only in the Do/w flow region at higher water cuts ( $\lambda_w > 0.875$ ). However, the model over-predicts the measured pressure gradient, in accordance with the results presented by Rodriguez et al. (2006). At higher water cuts the oil phase is completely dispersed in the water phase. Hence, the homogeneous model based on volume averaged mixture viscosity gives acceptable results. A large mismatch is observed when the water cut is below 0.875 where Do/w&w flow pattern is observed. Do/w&w flow pattern presents features of both stratified and dispersed flows. Therefore the predicted pressure drops based on homogeneous model deviate significantly from the measured data when the water cut is below 0.875. Hence, the predictions based on simple homogeneous model can not capture the complex behaviour of the measured pressure profile at higher water cuts. Therefore in order to model the complex behavior of the mixture viscosity and pressure drop of oil-water flow, more detailed models should be incorporated.

## 5. Conclusions

Oil-water flows in horizontal and inclined pipes were investigated. The experiments were conducted in a 15 m long, 56 mm diameter, inclinable steel pipe using Exxsol D60 oil and water as test fluids. The



**Figure 20.** Comparison of predicted and experimental pressure gradients for dispersed oil-water flow in horizontal pipe at  $U_m=1.50$  m/s.

test pipe inclination was changed in the range from  $5^\circ$  upward to  $5^\circ$  downward. The experiments were performed at different mixture velocities and water cuts. Mixture velocity and inlet water cut varies up to 1.50 m/s and 0.975, respectively. The time averaged cross sectional distributions of oil and water were measured with a traversable single-beam gamma densitometer. The pressure drop along the test section of the pipe was also measured. The characterization of flow patterns and identification of their boundaries was achieved via visual observations and analysis of local water volume fraction measurements. The following main conclusions can be drawn from this experimental study:

- The observed flow regimes of oil-water flow in horizontal and inclined pipes are categorized into eight different flow patterns, in accordance with the results presented by Trallero et al. (1997), Rodriguez et al. (2006) and Lum et al. (2006).
- The different flow patterns observed in oil-water flow are presented in terms of flow pattern maps for different pipe inclinations. In inclined flows the dispersion appears at lower mixture velocities than in horizontal flows. Smoothly stratified flow is observed in horizontal and downwardly inclined ( $-1^\circ$ ) pipes at low mixture velocities and intermediate water cuts. The stratified wavy flow regime is specially observed in upwardly inclined flows. However, this flow pattern completely disappears in downwardly inclined flows. Plug flow is observed at low mixture velocities for higher inlet water cuts in upwardly inclined flows. The Do/w and Do/w&w flow regimes extend towards lower water cuts as the pipe inclination is increased upwardly, due to the increased in situ water fraction. In addition, Dw/o flow regime shrinks towards lower water cuts as the pipe is upwardly inclined. The area occupied by the Do/w&w and Do/w flow regimes are extended towards lower water cuts and lower mixture velocities in downwardly inclined flows compared to the horizontal flows probably because of increased water velocity in downward inclinations and tendency of the water to disperse the oil. The Dw/o flow pattern is also observed at lower mixture velocities for downwardly inclined flows compared to the horizontal and upwardly inclined flows. The Do/w&w/o flow regime shrinks as the mixture velocity increases both in upwardly and downwardly inclined flows. The present observations on flow patterns show a good consensus with previous investigations.
- The local water volume fraction measurements are compared for different mixture velocities, inlet water cuts and pipe inclinations. In general, upward inclination results higher water hold-up than in horizontal flows due to gravitational forces. The water hold-up increases

significantly as the pipe inclination increases at lower mixture velocities. However, at higher mixture velocities the increase is moderated by increased flow momentum. Downwardly inclined flows result lower water hold-up compared to the horizontal flows.

- The frictional pressure drop is presented as a function of inlet water cuts for different mixture velocities for horizontal flows. A peak in pressured drop is observed at highre water cuts and shifts towards lower water cuts as the mixture velocity increases. This is attributed to the dispersion effect of the oil layer at higher water cuts, in accordance with the results presented by Nädler et al. (1997) and Elseth (2001). A drop in frictional pressure drop is obsevered at higher mixture velocities and lower water cuts due to drag reduction effect of oil-continuous dispersed flow.
- The measured water hold-up and pressure drop data are compared with two simple flow pattern dependent models, the two-fluid model for segregated flow and homogeneous model for dispersed flow. The two-fluid model gives better predictions for pressure drop and water hold-up at low mixture velocities when the phases are fully segregated. The homogeneous model gives better predictions of pressure drop of dual continuous flow compared to the two-fluid model. However, both models overestimates the pressure drop of dual continous flow. The homogenous model over-predicts the pressure drop of Dw/o and Do/w flows. A large mismatch is observed between model predictions and measured pressure drop in Do/w&w flows. Hence, more detailed models should be incorporated to predict flow properties of oil-water flows.

## 6. References

- Abduvayt P, Manabe R, Watanabe T and Arihara N 2004 Analysis of oil–water flow tests in horizontal, hilly-terrain and vertical pipes *In: Proc. Annual SPE Tech. Conf., Houston, Texas (SPE 90096), in CD ROM*
- Alkaya B 2000 Oil–water flow patterns and pressure gradients in slightly inclined pipes *M.S. Thesis, The University of Tulsa, USA*
- Angeli P 1996 Liquid-liquid dispersed flows in horizontal pipes *PhD Thesis. (Imperial College of science, technology and medicine, London SW7 2BY)*
- Angeli P and Hewitt G F 1998 Pressure gradient in horizontal liquid-liquid flows *Int. J. Multiphase Flow*. **24** 1183-1203
- Brauner N and Maron M D 1989 Two-phase liquid-liquid stratified flow *PhysioChemical Hydrodynamics* **11** No 4 487-506
- Chan A M C and Banerjee S 1981 Design aspects of gamma densitometers for void fraction measurements in small scale two-phase flows *Nuclear Instruments and Methods* **190** 135-148
- Chaoki J, Larachi F and Dudukovic M 1997 Non-invasive monitoring of multiphase flows *Elsevier, Amsterdam*
- Charles M E, Govier G W and Hodgson G W 1961 The horizontal pipeline flow of equal density oil-water mixture *Can. J. Chem. Eng.* **39** 27-36
- Charles M E and Lilleleht L U 1966 Correlation of pressure gradients for the stratified laminar-turbulent pipeline flow of two immiscible liquids *Can. J.Chem. Eng.* 9-17
- Cox A L 1985 A study of horizontal and downhill two-phase oil–water flow *M.S. Thesis, University of Texas at Austin, USA*
- Elseth G 2001 An experimental study of oil-water flow in horizontal pipes *PhD Thesis, The Norwegian University of Science and Technology, Norway*
- Flores J G, Sarica C, Chen X T and Brill J P 1998 Investigation of hold-up and pressure drop behaviour for oil-water flow in vertical and deviated wells *Trans. ASME J. Energy Resour. Tech.* **120** 8-14
- Guzhov A I, Grishan A L, Medredev V F and Medredeva O P 1973 Emulsion formation during the flow of two immiscible liquids in a pipe *Neft.* **8** 58-61



- Hardin S 1995 The viscosity of stable and unstable oil-water emulsions and the comparison of the UK National Multiphase Flow Database with oil-water-gas flow models of pipelines *A link project report, Imperial college, London*
- Huang S F, Zhang X G, Wang D and Lin Z H 2007 Water hold-up measurement in kerosene–water two-phase flows *Meas. Sci. Technol.* **18** No 12 3784-3794
- Lockhart R W and Martinelli R C 1949 Proposed correlation of data for isothermal two-phase, two-component flow in pipes *Chem. Eng. Prog.* **45** No 1 39-48
- Lovick J and Angeli P 2004 Droplet size and velocity profiles in liquid-liquid horizontal flows *Chem. Eng. Sci.* **59** 3105-3115
- Lum J Y L, Al-Wahaibi T and Angeli P 2006 Upward and downward inclination oil-water flows *Int. J. Multiphase Flow.* **32** 413-435
- Lum J Y L, Lovick J and Angeli P 2004 Low inclination oil–water flows *Canad. J. Chem. Eng.* **82** 303–315
- Malinowsky M S 1975 An experimental study of oil-water and air-oil-water flowing mixtures in horizontal pipes *M.S. Thesis, The University of Tulsa, USA.*
- Nädler M and Mewes D 1997 Flow induced emulsification in the flow of two immiscible liquids in horizontal pipes *Int. J. Multiphase Flow* **23** 55–68
- Oddie G, Shi H, Durlfosky L J, Aziz K, Pfeffer B and Holmes J A 2003. Experimental study of two and three phase flows in large diameter inclined pipes *Int. J. Multiphase Flow* **29** 527–558.
- Oglesby K D 1979 An experimental study on the effect of oil viscosity, mixture, velocity and water fraction on horizontal oil-water flow *MS Thesis University of Tulsa*
- Pal R 1993 Pipeline flow of unstable and surfactant-stabilized emulsions *AIChE J.* **39(11)** 1754-1764
- Rodriguez O M H and Oliemans R V A 2006 Experimental study on oil-water flow in horizontal and slightly inclined pipes *Int. J. Multiphase Flow.* **32** 323-343
- Russel T W F, Hodgson G W and Govier G W 1959 Horizontal pipeline flow of mixtures of oil and water *Can. J. Chem. Eng.* **37**, 9-17
- Scott G M 1985 A study of two-phase liquid–liquid flow at variable inclinations *M.S. Thesis, University of Texas at Austin, USA*
- Soleimani A, Lawrence C J and Hewitt G F 1997 Effect of mixers on flow pattern and pressure drop in horizontal oil-water pipe flow *International symposium on liquid-liquid two-phase flow and Transport phenomena, ICHMT, Antalya, Turkey*
- Soleimani A 1999 Phase distribution and associated phenomena in oil-water flows in horizontal tubes *PhD Thesis, Imperial College, University of London*
- Taitel Y and Dukler A E 1976 A model for predicting flow regime transitions in horizontal and near horizontal gas-liquid flow *AIChE Journal.* **22** 47-55
- Trallero J L, Sarica C and Brill J P 1997 A study of oil-water flow patterns in horizontal pipes *SPE Production & Facilities* 165-172
- Valle A 1998 Multiphase pipeline flows in hydrocarbon recovery *Multiphase Science and Technology* **10** 1-139
- Valle A and Kvandal H K 1995 Pressure drop and dispersion characteristics of separated oil-water flows *International symposium on Two-phase flow modelling and experimentation, Rome*
- Valle A and Utvik O H 1997 Pressure drop, flow pattern and slip for two-phase crude oil-water flow: Experiments and model predictions *International symposium on liquid-liquid two-phase flow and Transport phenomena, ICHMT, Antalya, Turkey*
- Vigneaux P, Chenais P and Hulin J P 1988 Liquid-liquid flows in an inclined pipe *AIChE Journal* **34** 781-789